

Experimental study on the effect of penetration length and eccentricity of sheet pile foundation on bearing capacity

R. Shikakura

Graduate School of Science and Engineering, Chuo University, Tokyo, Japan

H. Nishioka

Department of Civil and Environmental Engineering, Chuo University, Tokyo, Japan

Y. Yamakuri

Department of Civil and Environmental Engineering, Chuo University, Tokyo, Japan

Y. Arai

Department of Civil and Environmental Engineering, Chuo University, Tokyo, Japan (Former)

M. Hirano

Graduate School of Science and Engineering, Chuo University, Tokyo, Japan

ABSTRACT

Sheet pile foundations is an innovative combined type of foundation that directly integrates sheet piles (SP), typically used for temporary earth-retaining, with a footing. Sheet pile foundations are more cost-effective than traditional pile foundations and can be versatile across various ground conditions than the shallow foundation. Additionally, the sheet pile reinforcement method is what sheet pile foundation technology applies to. Previous studies have proposed a head-connection type for this method, where the footing and SP are not fully integrated. However, the required penetration length of the SP and its effect under eccentricity remain insufficiently understood. In this study, we conducted vertical loading experiments using a 2D ground model composed of aluminum rods, and varying the SP penetration length and eccentricity from the center of gravity. Image analysis was employed to track the movement of the model's ground particles and to visualize slip lines. As a result, the bearing capacity is improved by penetrating the SP. In particular, it is suggested that there is an optimal penetration length, akin to the breadth of the shallow foundation, crucial for maximizing reinforcement effectiveness. Furthermore, even under conditions of increased eccentricity, SP reinforcement demonstrated enhanced bearing capacity compared to shallow foundations.

Key words: *Sheet pile foundation, Ultimate Bearing capacity, Aluminum rods, Eccentricity, Image Analysis*

1. Background and objectives of the study

Following the 1995 Southern Hyogo Prefecture Earthquake, seismic design standards for structures underwent significant improvements. Although these new standards apply to foundation structures, many are still based on previous seismic design standards. Therefore, the sheet pile reinforcement method, rooted in sheet pile foundation technology, has been proposed to reinforce shallow foundations.

The sheet pile foundation (Nishioka, 2017) is a novel

combined foundation type that directly integrates sheet piles (SP) used for temporary earth-retaining with footings. **Fig. 1** illustrates a sketch that compares the sheet pile foundation with the shallow foundation (Nishioka, 2010). As opposed to the conventional shallow foundation (a), the sheet pile foundation (b) does not require removal of SP, which are combined to the footing. Also, it is more economical than pile foundations and applicable to a wider range of ground conditions than the shallow foundation. Whereas the shallow foundation's

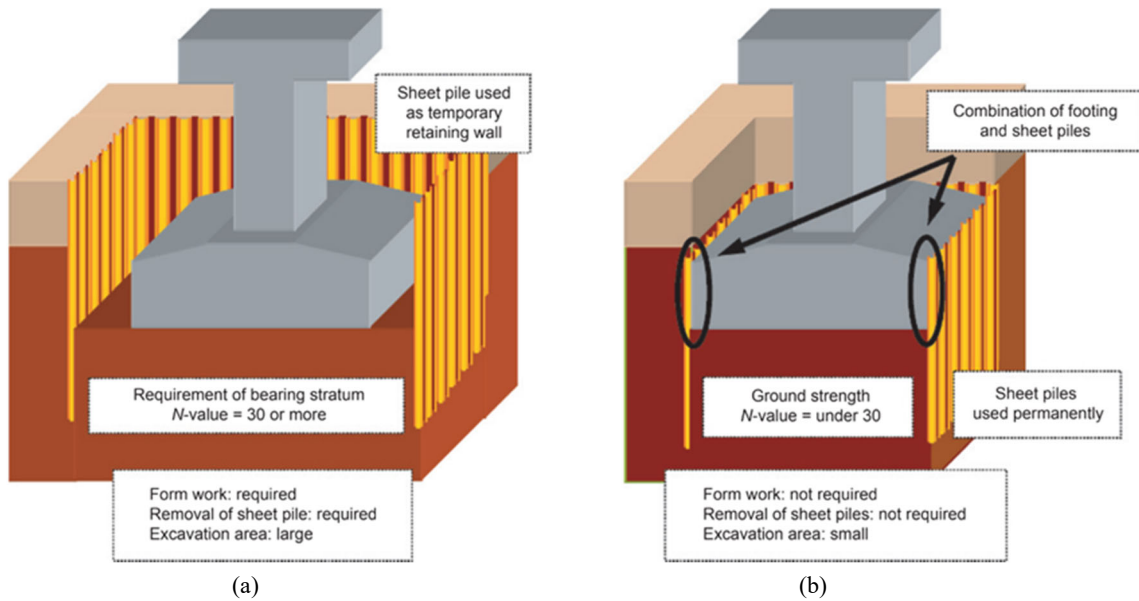


Fig. 1 Outline of sheet pile foundation: (a) conventional shallow foundation; (b) sheet pile foundation (Nishioka, 2010)

requirement of bearing stratum is N -value = 30 or more, the sheet pile foundation is expected to apply the ground whose N -value = under 30.

The sheet pile reinforcement method is what sheet pile foundation technology applies to. In this method, the SP are pressed around an existing structure. The sheet pile reinforcement method does not require large machinery for installation, enabling installation in limited spaces. Additionally, it reduces environmental impact due to the low amount of construction soil. This approach is economical as it only requires SP for reinforcement, enhancing vertical and horizontal bearing capacity and seismic resistance by restraining the ground and suppressing strain localization. Previous studies (Nishioka, 2004) proposed a head-connection type where the footing and SP are not completely integrated, with the head closed only with concrete. However, quantitative studies are insufficient in the current design model. In particular, the required penetration length of the SP and its effect under eccentricity remain unclear. Thus, in this study, vertical loading experiments were conducted using a 2D ground model, varying the SP penetration length and eccentricity from the foundation's center of gravity. The study investigated the effects of sheet pile reinforcement on vertical bearing capacity and the influence of eccentricity by measuring ultimate bearing capacity.

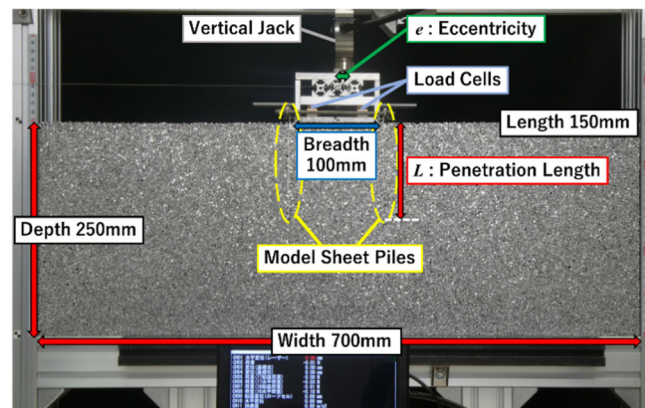


Fig. 2 Model ground and experimental devices

2. Outline of the Experiment

2.1. Aluminum rods ground model

The ground model and experimental devices utilized in this study are depicted in **Fig. 2**. We employed a ground model comprising aluminum rods to replicate dry sandy conditions. The internal friction angle ϕ was estimated as 27.8° by comparing the results of the vertical loading tests (CaseL0) and Terzaghi's bearing capacity formula (**Eq. (1) ~ (3)**). Also, it is estimated that ϕ is between $25\sim 30^\circ$ by the angle of repose test.

$$q_u = \gamma D_f N_q + \frac{1}{2} \gamma B N_\gamma \quad (1)$$

$$N_\gamma = (N_q - 1) \tan(1.4\phi) \quad (2)$$

$$N_q = \tan^2\left(\frac{\pi}{4} + \frac{\phi}{2}\right) e^{\pi \tan \phi} \quad (3)$$

where, q_u : ultimate bearing capacity (kN/m^2), γ : unit weight (kN/m^3), D_f : embedded depth (m), N_q and N_γ : bearing capacity factors, B : breadth of the shallow foundation (m).

An advantage of using Aluminum rods ground model is that it allows aluminum rods to be photographed from the side, facilitating observation of displacement and deformation through image analysis. Furthermore, because particle characteristics remain consistent even after repeated experiments, ensures high experimental reproducibility.

For the soil tank, we used a stack of 150 mm-long aluminum rods arranged to a width of 700 mm and a height of 250 mm. The aluminum rods had diameters of 1.5, 2, and 3 mm and were mixed with a weight ratio of 1:1:1. This ratio results in a particle size accumulation curve nearly parallel to that of Toyoura sand. The ground model was loosely packed, with a unit weight of approximately 21.1 kN/m^3 .

2.2. Experimental devices

The dead load of the shallow foundation model (SF) measured 23.1 N, with a breadth of 100 mm, corresponding to a 1/50 scale of a real shallow foundation with a 4.8 m breadth. Loading persisted until the vertical jack's displacement exceeded 10 mm (10% of the SF's breadth) using the vertical jack, equipped with a roller to prevent interference with SF rotation and horizontal displacement. Fig. 3 illustrates a schematic of the experimental device as seen from the rear of Fig. 2. Leveraging the characteristics of the self-supporting ground model, two laser displacement sensors were installed behind the soil tank to measure the vertical displacement and the photograph is shown in Fig. 4. They were affixed 30 mm from both sides of the SF center. Loads were gauged using two load cells attached on the SF's bottom and one on the jack. The horizontal displacement at the SF's bottom was computed using a wire-type horizontal displacement meter, and an accelerometer which was installed to measure the SF's rotation angle.

2.3. Penetration of the sheet piles

Fig. 5 illustrates the aluminum plates employed to simulate the sheet piles (SP) and their fixing devices. The aluminum plate, with a Young's modulus E of 73 kN/m^2 ,

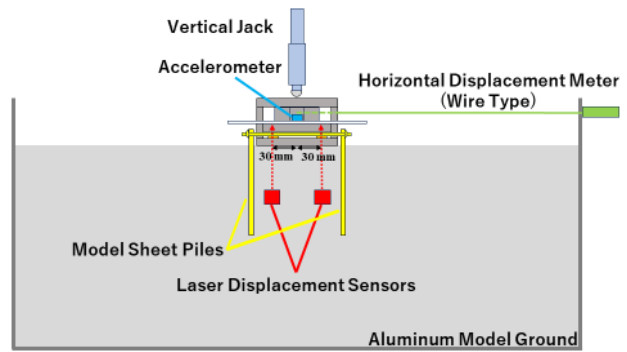


Fig. 3 Experimental devices (rear view of Fig. 2)



Fig. 4 Two laser displacement sensors

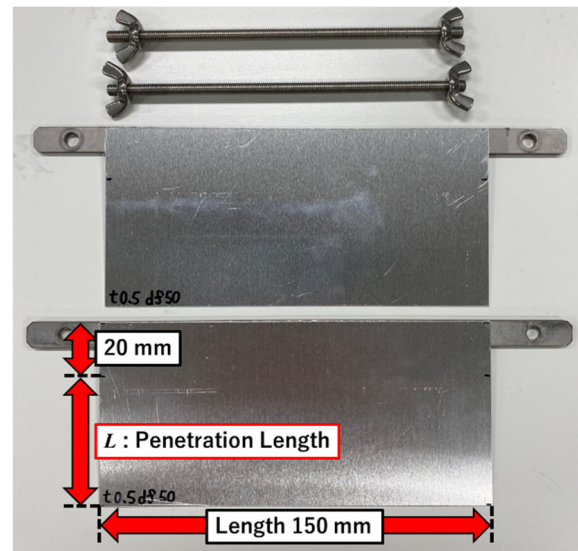


Fig. 5 Model SP and its fixing devices (in Case of $L = 50\text{mm}$)

has a thickness of 0.5 mm and a length of 150 mm, matching the aluminum rods' length. SP penetration into the model ground occurred with a specified penetration length L , and the upper parts protruded 20 mm. The upper sections of the SP were connected to fully threaded rods and wing nuts to fix the distance between the left and right SP at the top. Since the SF and SP did not make contact,

Table 1. Experiment cases varying L

L : Penetration Length of SP	βL	Case
0 mm (Not SP)		CaseL0
20 mm	0.57	CaseL20
50 mm	1.42	CaseL50
80 mm	2.28	CaseL80
110 mm	3.13	CaseL110
140 mm	3.99	CaseL140

only the SF settled under load, with no load transmitted to the SP. This corresponds to the head-connected type of sheet pile reinforcement method. In all experimental cases, the SP exhibited no plastic deformation and behaved within the elastic deformation range.

2.4. Experimental cases

In this study, vertical loading experiments were conducted, varying the penetration length of the sheet pile SP L , and the eccentricity from the center of gravity e .

The cases with varying penetration lengths are outlined in **Table 1**. Six penetration lengths were considered: 0 (without SP), 20, 50, 80, 110, and 140 mm. Each experimental case was repeated three times to account for result variability. To match the relative ratio of SP and soil stiffness, a dimensionless quantity expressing the relative ratio of pile stiffness to penetration length, βL , was used as an index. It was calculated using **Eq. (4)**, incorporating the coefficient of the horizontal subgrade reaction (2000 kN/m³) of the aluminum model ground, obtained separately from the horizontal loading experiment conducted on the SP alone. For the actual SP on loosely packed ground with a rooting length equal to the SF breadth, $\beta L = 2.84$, so the rigidity is approximately similar to the actual one.

$$\beta L = \sqrt[4]{\frac{Bk_h}{4EI}} \times L \tag{4}$$

where β : characteristic value of the pile (m⁻¹), L : penetration length of the SP (m), B : ground model length (0.15 m), k_h : coefficient of horizontal subgrade reaction (kN/m³), E : Young's modulus (7.3×10^7 kN/m²), I : second moment of the area (m⁴).

The cases varying the eccentricity e are listed in **Table 2**. In addition to the cases without SP penetration, the penetration lengths of the SP were set at 80 and 110 mm, close to the breadth of the SF. The eccentricity e

Table 2. Experiment cases varying e

e : Eccentricity		$L = 0$ mm (Not SP)	$L = 80$ mm	$L = 110$ mm
0	0 mm	CaseL0	CaseL80	CaseL110
$B/12$	8.3 mm	CaseL0e8.3	CaseL80e8.3	CaseL110e8.3
$B/6$	16.7 mm	CaseL0e16.7	CaseL80e16.7	CaseL110e16.7
$B/4$	25 mm	CaseL0e25	CaseL80e25	CaseL110e25

※ B is breadth of the shallow foundation model (100 mm)

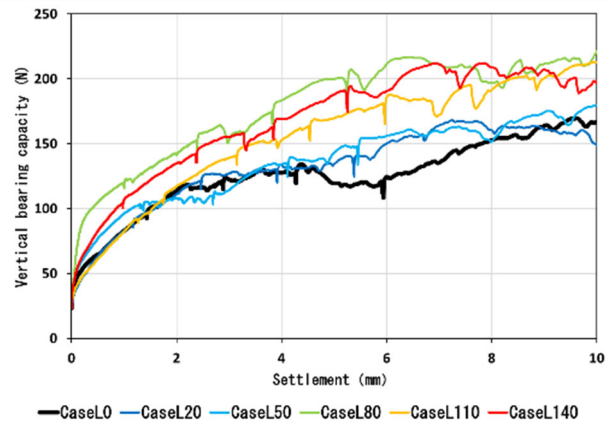


Fig. 6 Load-settlement curve

varied by 0, 8.3, 16.7, and 25 mm. In particular, $e = 16.7$ mm corresponds to $B/6$, which is the amount of eccentricity that theoretically causes the uplift of the bottom of the SF. We observed any changes in the failure mode of the ground when setting lower and higher eccentricity values. Like in the cases with varying penetration lengths, the experiments were repeated three times for each experimental case to account for variations in the ultimate bearing capacity.

3. Experimental results

3.1. Results for varying penetration lengths L

The load-settlement curves for different penetration lengths are depicted in **Fig. 6**. Among the three tests conducted, the one where the ultimate bearing capacity (maximum capacity until settlement reached 10% of the shallow foundation (SF)'s breadth) was intermediate taken as the representative value. It is evident that the SP with penetration lengths of 20 and 50 mm had a negligible effect on bearing capacity compared to cases without SP. However, for lengths over 80 mm, both the coefficient of subgrade reaction and bearing capacity exhibited an increase.

The relationship between the penetration length of

the SP L and the ultimate bearing capacity for all experiments is plotted in Fig. 7. The points on the orange line indicate the average values of the three ultimate bearing capacities achieved for each case. The bearing capacity increased by 24.3%, from 171.5 N in Case L0 to 213.2 N in Case L80. The plateauing tendency in ultimate bearing capacity suggests an optimal penetration length for the most effective reinforcement. However, the improvement effect on bearing capacity was minimal with increased penetration length, and little improvement was observed with too short penetration lengths.

In addition, assuming that the SF have embedded depth D_f and the results were compared with the SF's penetration length. The estimated line is drawn in Fig. 7 and it is calculated from Eq. (1) ~ (3). Here, $N_q = 14.42$ and $N_\gamma = 10.84$. Comparing them on the same scale, it turns out there's big difference.

To track ground particle movement and visualize slip lines, image analysis was conducted, as shown in Fig. 8. The ground displacement is at a 10 mm settlement of the vertical jack, with indicated positions of slip lines (white lines) and the SP (yellow lines). Beyond $L=80$ mm, the slip line deepened and the slip area significantly expanded as the penetration length of the SP increased. Additionally, the SP underwent elastic deformation, believed to enhance bearing capacity by impeding ground particle movement. Notably, the penetration length of SP $L = 80$ mm closely matched the maximum depth of the slip line in Case L0. Consequently, substantial bearing capacity improvement is achievable by penetrating the SP to the depth of the slip line when utilizing only a SF.

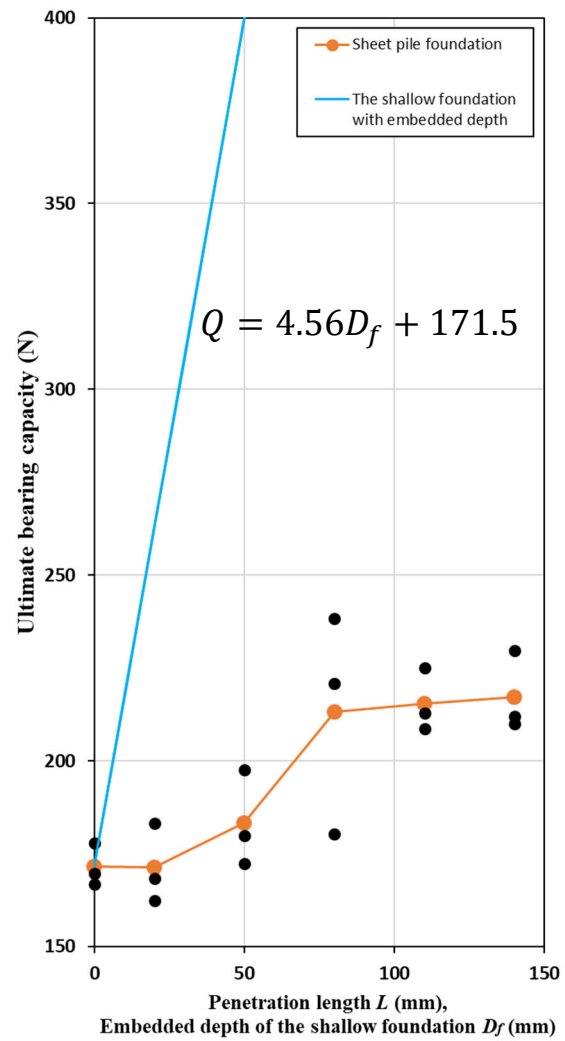


Fig. 7 Relationship between L and ultimate bearing capacity

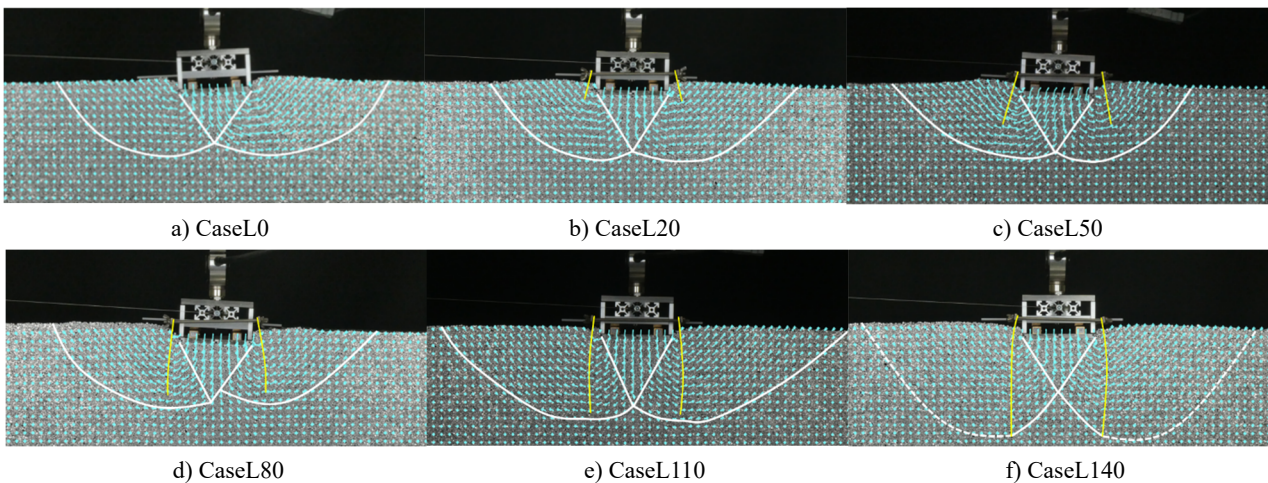


Fig. 8 Image analysis results with varying SP penetration lengths

3.2. Results for varying eccentricities e

In the experiment, four different eccentricities were initially provided by varying the eccentricity. However, as the SF settled, the eccentricity at the bottom changed. Therefore, the eccentricity at ultimate bearing capacity was calculated using Eq. (5), where the bending moment M was obtained from the two load cells at the bottom.

$$e_b = \frac{M}{V} \quad (5)$$

where e_b : eccentricity at the bottom of the SF (mm), M : moment at the bottom of the SF(N·mm), V : vertical load (N).

The relationship between the eccentricity computed with Eq. (5) and the ultimate bearing capacity is presented in Fig. 9. It is evident that SP reinforcement effectively improves the bearing capacity even under eccentric loads. The relationship between eccentricity and ultimate bearing capacities for penetration lengths of $L = 80$ mm and $L = 110$ mm remains consistent as long as the eccentricity is not excessively large, suggesting sufficient reinforcement effect with the required SP penetration length.

Similar to 3.1, image analysis was conducted, and the results are depicted in Fig. 10. Initially, for the case of only SF, a wedge-shaped area occurs up to an eccentricity of $B/6$ (16.7 mm), theoretically causing bottom uplifting. Beyond this value, the wedge-shaped area disappears, and the failure mode shifts to an arc slip. However, at $L = 80$

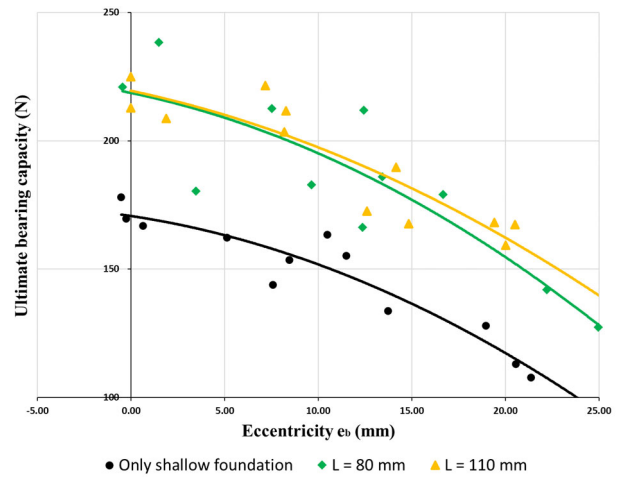


Fig. 9 Relationship between e_b and ultimate bearing capacity

mm and $L = 110$ mm no wedge-shaped area was observed even after a slight eccentricity. Instead, a slip line with depth close to the SP penetration depth occurred, attributed to ground particle resistance in unison with the SP. Additionally, displacement on the loaded side was suppressed by the right SP. Although the slip area was larger at $L = 110$ mm than at $L = 80$ mm, there was no significant increase in bearing capacity.

4. Conclusion

The following conclusions can be drawn from the results of the 2D model experiments on the head connection type of the SP reinforcement method.

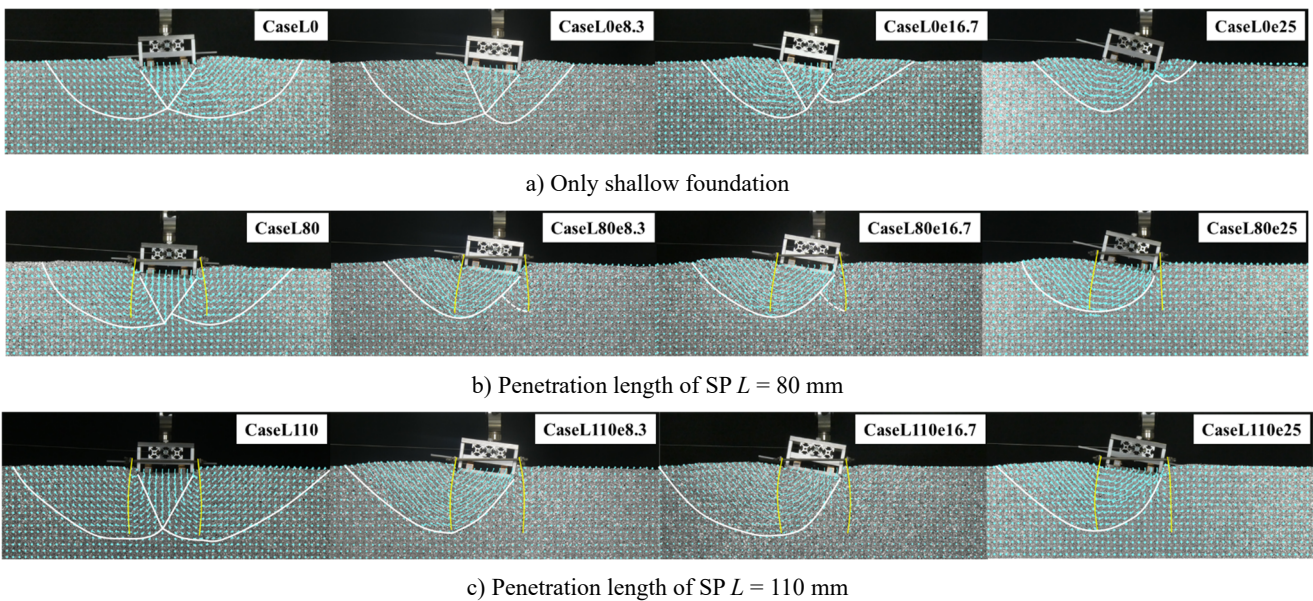


Fig. 10 Image analysis results with varying eccentricity

- 1) Penetrating the SP which length is akin to the shallow foundation (SF)'s breadth, significantly improves the bearing capacity. Emphasizing an optimal penetration length close to the breadth of the SF enhances reinforcement effectiveness.
- 2) The improvement in bearing capacity was limited when the penetration length was longer than the optimal penetration length, and almost no improvement was observed when the penetration length was too short.
- 3) A significant enhancement in the bearing capacity can be achieved by penetrating the SP that reaches the maximum depth of the slip line, which can be observed in cases where only a SF is used.
- 4) Even under conditions of increased eccentricity, SP reinforcement demonstrated enhanced bearing capacity compared to SF.
- 5) Under eccentric loading, displacement on the loaded side is suppressed, while on the opposite of the loaded side, the SP and ground particles tend to resist together.

In future endeavors, we will further investigate the effects of the SP reinforcement by varying the fixation conditions and conducting combined loading tests representative of earthquakes.

5. Acknowledgements

We would like to thank Editage (www.editage.jp) for English language editing.

References

- Nishioka, H., 2017. Development of Sheet pile foundation. IPA News Letter, 2(4), pp. 13-16.
- Nishioka, H., Koda, M., Hirao, J., and Higuchi, S., 2010. Vertical and combined loading tests for sheet pile foundation. International Journal of Physical Modelling in Geotechnics 10, No.2, 25-34.
- Nishioka, H., Koda, M., Murata, O., Matsuda, T., and Hirao, J., 2004. Experimental research on the method to joint sheet piles to a footing of sheet-pile foundation. Proceedings of the Geotechnical Engineering Symposium, pp. 275-282. (in Japanese)